www.sciencetranslationalmedicine.org/cgi/content/full/4/124/124ra27/DC1

Supplementary Materials for

Fasting Cycles Retard Growth of Tumors and Sensitize a Range of Cancer Cell Types to Chemotherapy

Changhan Lee, Lizzia Raffaghello, Sebastian Brandhorst, Fernando M. Safdie, Giovanna Bianchi, Alejandro Martin-Montalvo, Vito Pistoia, Min Wei, Saewon Hwang, Annalisa Merlino, Laura Emionite, Rafael de Cabo, Valter D. Longo*

*To whom correspondence should be addressed. E-mail: vlongo@usc.edu

Published 7 March 2012, *Sci. Transl. Med.* **4**, 124ra27 (2012)
DOI: 10.1126/scitranslmed.3003293

The PDF file includes:

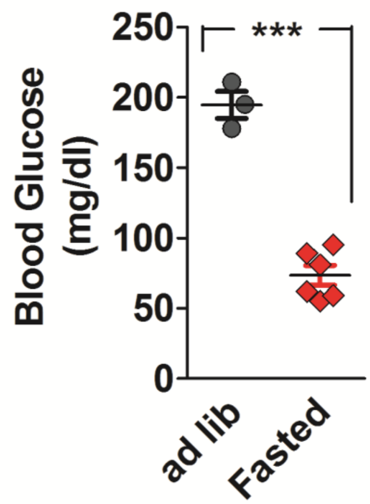

Fig. S1. The effect of 48-hour fasting on blood glucose levels in mice. Student's *t*-test, ***$P<0.001$ (N=3-6).

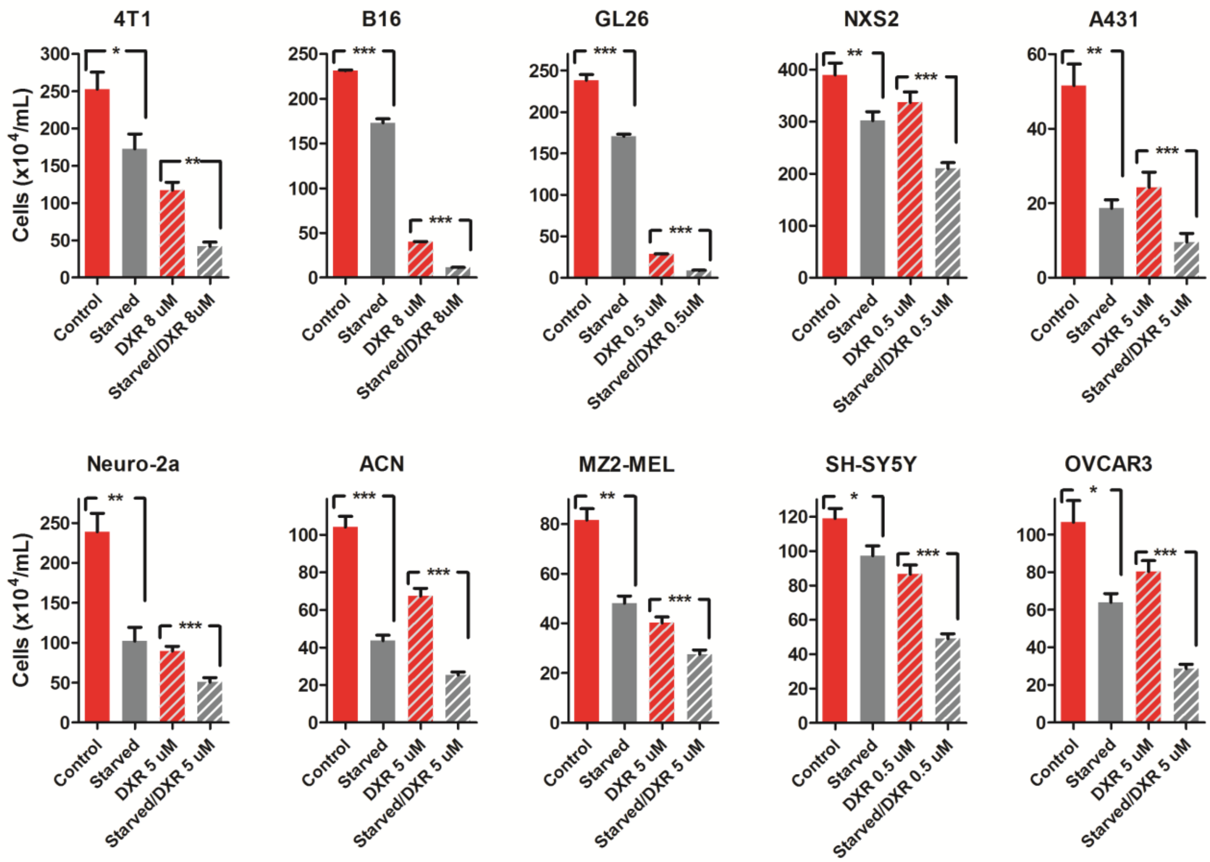

Fig. S2, related to Fig. 1 and Fig. S2A. Cell viability after starvation and DXR was confirmed by trypan blue exclusion. (N=3) Student's *t*-test, **P*<0.05, ***P*<0.01, ****P*<0.001.

A

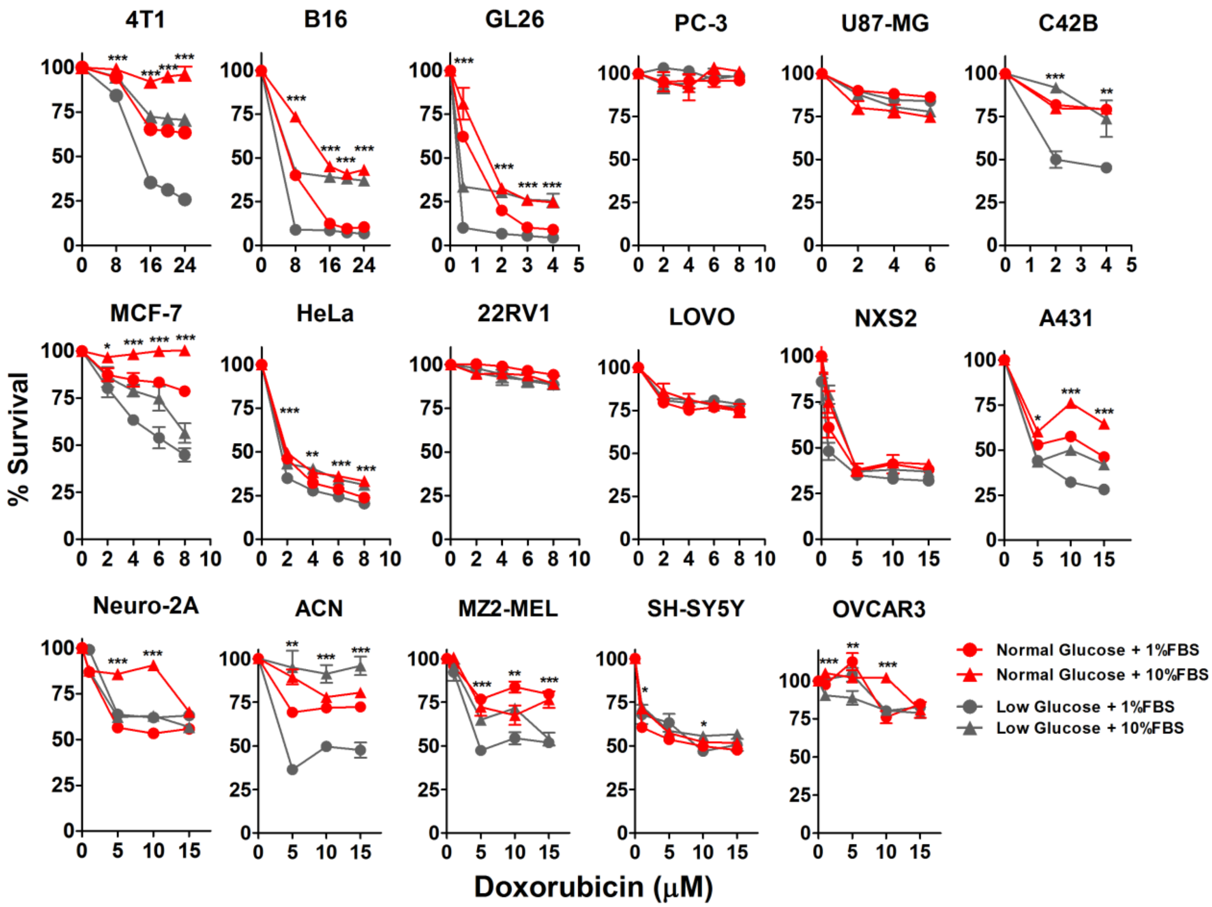

4T1
B16
GL26
PC-3
U87-MG
C42B
MCF-7
HeLa
22RV1
LOVO
NXS2
A431
Neuro-2A
ACN
MZ2-MEL
SH-SY5Y
OVCAR3
% Survival
Doxorubicin (μM)
Normal Glucose + 1%FBS
Normal Glucose + 10%FBS
Low Glucose + 1%FBS
Low Glucose + 10%FBS

B

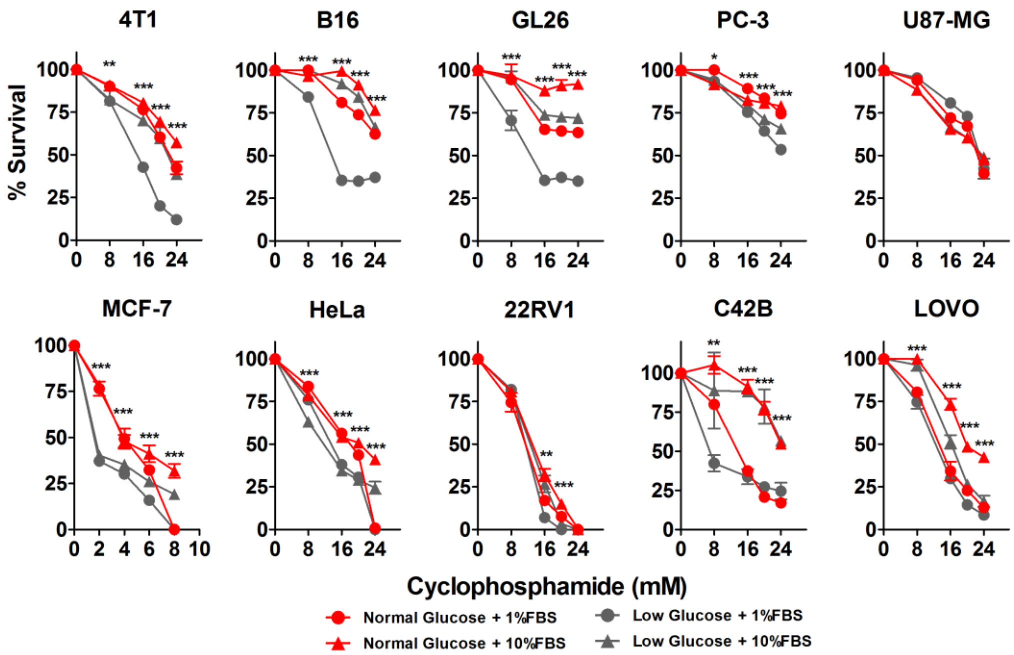

Fig. S3, related to Fig. 1. **Effect of starvation on DXR or CP sensitivity of 17 different cancer cell lines in vitro**. Fasting leads to glucose and growth factor reduction. To model this in vitro, we starved 4 different murine cancer cells - breast cancer (4T1), melanoma (B16), glioma (GL26), and neuroblastoma (NXS2 and Neuro-2a) - and also 13 different human cancer cells - prostate cancer (PC3, 22Rv1), breast cancer (MCF-7, C42B), glioblastoma (U87-MG), cervical cancer (HeLa), colon cancer (LOVO), neuroblastoma (ACN, SH-SY5Y), epidermoid carcinoma (A431), melanoma (MZ2-MEL) and ovarian cancer (OVCAR3) - and challenged with DXR or CP. Cells were cultured in normal glucose (1.0 g/L and 2.0 g/L glucose, for human and murine cells respectively), or low glucose (0.5g/L) supplemented with 1% or 10% FBS. Survival was determined by MTT reduction. (N=3-6). One-way ANOVA, *P<0.05, **P<0.01, ***P<0.001.

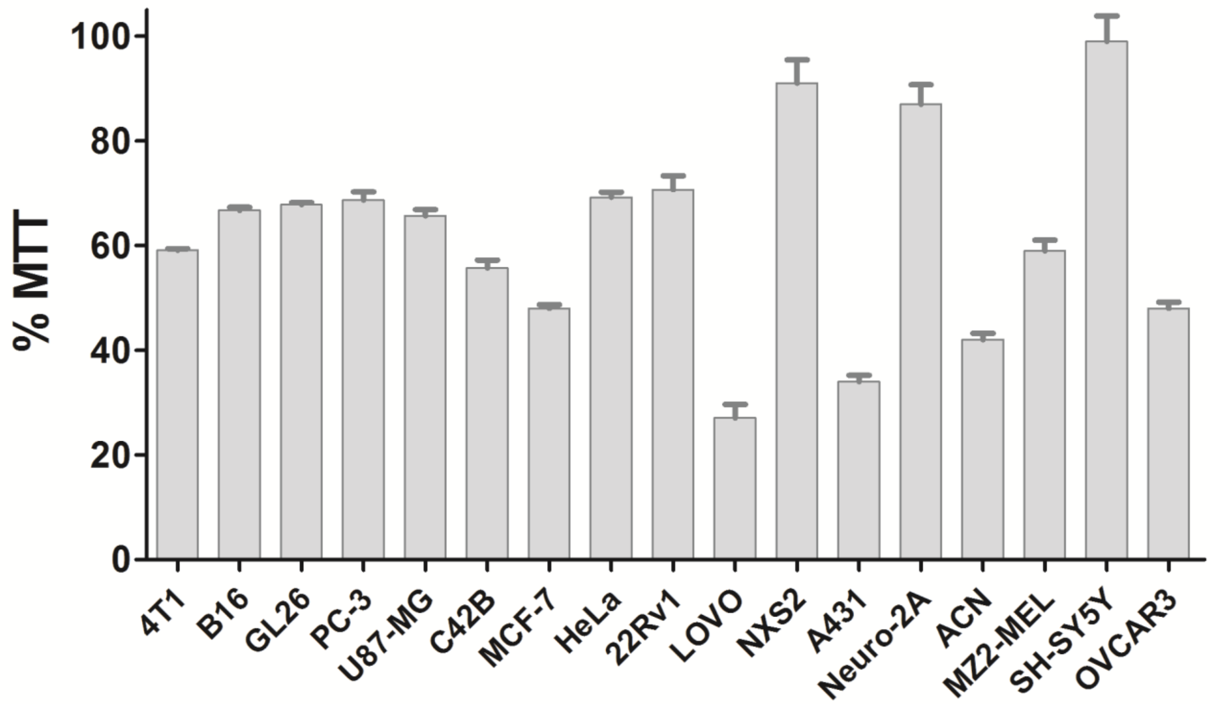

Fig. S4, related to Figs. 1 and S3. Effect of starvation alone on the sensitivity of 17 different cancer cell lines in vitro. Cells were cultured under starvation (0.5 g/L glucose, 1% FBS) or normal conditions (1.0 g/L and 2.0 g/L glucose, for human and murine cells respectively, 10% FBS) for 48-hours. Data shown as % MTT reduction of cells under starvation *vs* normal conditions (N=6-12).

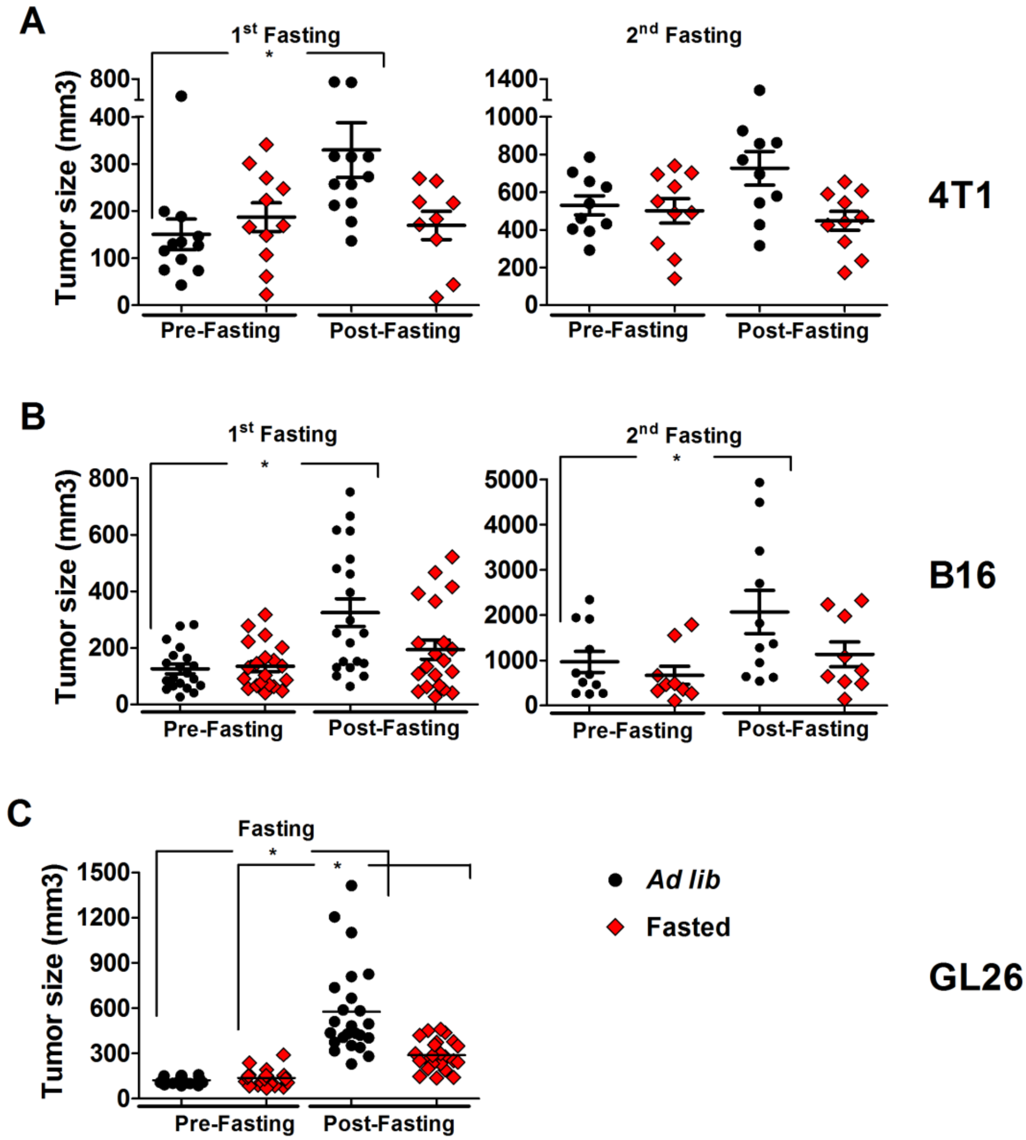

Fig. S5, related to Fig. 2. The effect of fasting on tumor progression. Fasting (48hours) retards the progression of subcutaneous tumors of mouse (A) breast cancer (4T1), (B) melanoma (B16), and (C) glioma (GL26). This figure shows detailed comparisons of tumor size immediately before and after fasting for 48 hours, as presented in Figure 2 A, C, E. Student's *t*-test, **P*<0.05.

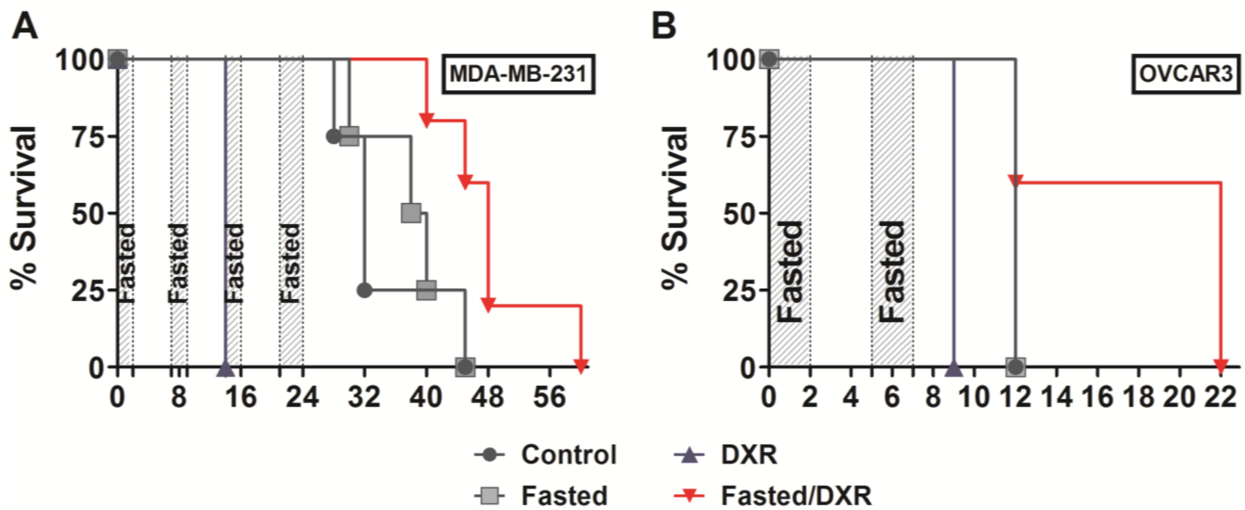

Fig. S6, related to Fig. 2. Effect of fasting on the survival of xenograft tumor mouse models treated with DXR. (A) Human breast cancer cells (MDA-MB-231) were subcutaneously injected into nude mice. 4 cycles of fasting (48 hours) and/or DXR were performed. Mice that were fed ad lib and treated with DXR died at day 14 for DXR toxicity (N=5). Log-rank test; control *vs* fasted (NS), DXR ($P<0.05$), fasted/DXR ($P<0.05$), DXR *vs* fasted/DXR ($P<0.01$), DXR *vs* fasted ($P<0.01$), fasted *vs* fasted/DXR ($P<0.05$). (B) Human ovarian cancer cells (OVCAR3) were subcutaneously xenografted into nude mice. 2 cycles of fasting (48 hours) and/or DXR were performed. Mice that were fed ad lib and treated with DXR were terminated at day 9 due to death of all mice from DXR toxicity (N=5). Log-rank test; control *vs* fasted (NS), DXR ($P<0.01$), fasted/DXR ($P<0.05$), DXR *vs* fasted/DXR ($P<0.01$), DXR *vs* fasted ($P<0.01$), fasted *vs* fasted/DXR ($P<0.05$).In both xenograft models, fasted mice treated with DXR did not experience toxicity.

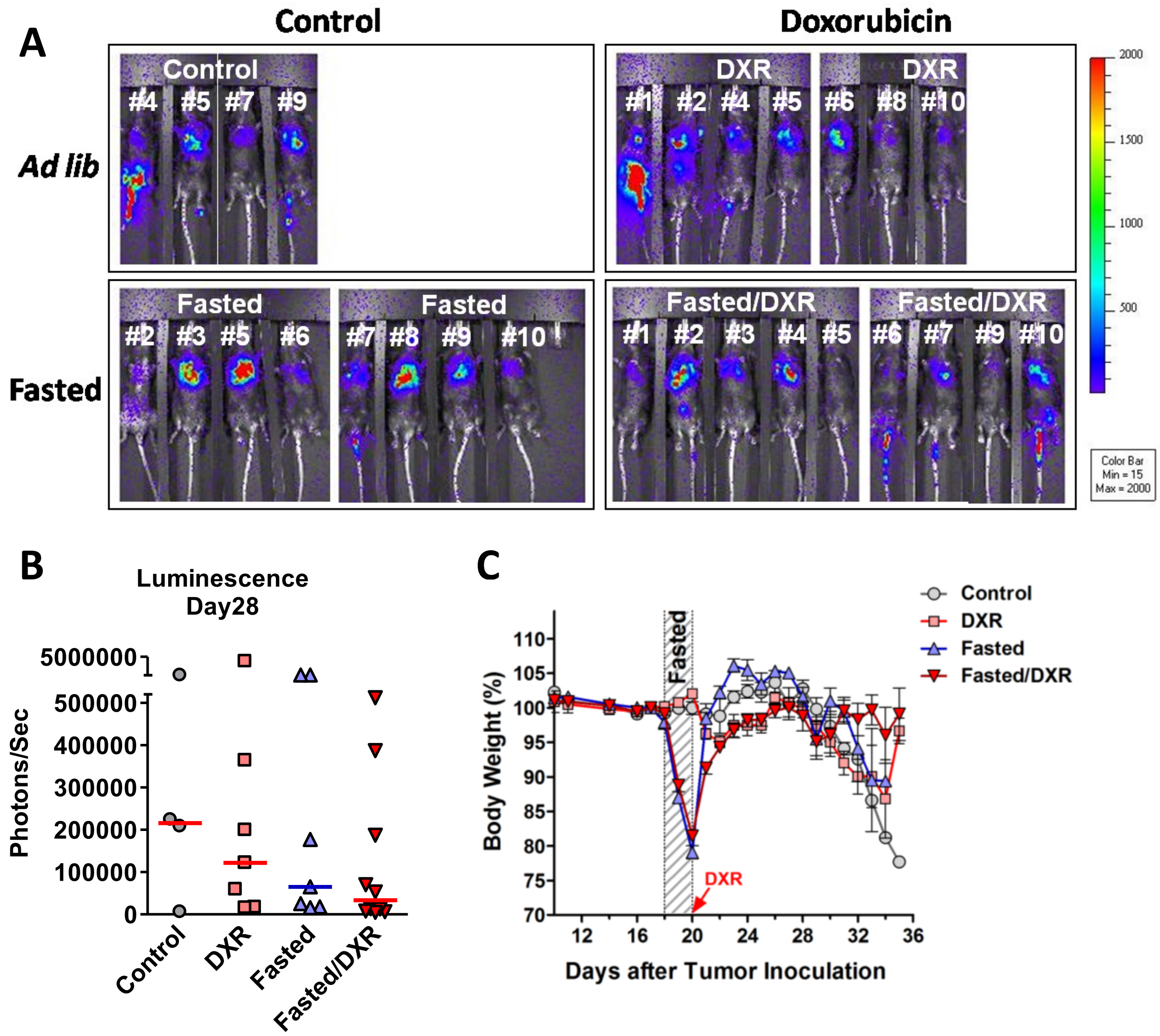

Fig. S7, related to Fig. 3. **Effect of fasting on tumor burden and the antitumor effect of DXR**. (A) Bioluminescence imaging (BLI) of the metastasized luciferase-tagged B16 melanoma cells 28 days following tumor injection and 1 cycle of fasting/DXR (N=10). Some mice from the control (n=1), DXR (n=3), and fasted/DXR (n=1) group did not show adequate metastasis and thus were not included in the figure. (B) Quantification of (A). (C) Body weight lost during fasting was rapidly recovered upon normal feeding.

Cytosolic Ribosome	rRNA Binding	Ribosome Biogenesis		Translation				Cytosolic Large Ribosomal Subunit
EIF2A	A	2410016O06RIK	NOL14	A	GFM1	MTRF1	RPS24	RPL19
RPL12	ANG	A	NOL5	AARS	GSPT1	NACA	RPS26	RPL3
RPL21	BXDC5	AATF	NOL5A	AARS2	HARS	NARS	RPS27A	RPL37
RPL22	IMP3	BC003885	NOLA1	AARSD1	HBS1L	NARS2	RPS27L	RPL39
RPL23	MRPS17	BMS1	NOLA2	ABCF1	IARS	NCOA5	RPS3	RS1
RPL27	NOL1	BOP1	NOLA3	ABTB1	IARS2	NOLA2	RPS3A	ZCCHC17
RPL28	NOL12	BXDC2	OTT	ALDH1L1	IMP3	OTT	RPS4X	
RPL29	NOLA1	BXDC5	PES1	BC003885	KARS	PARS2	RPS4Y2	
RPL3	NPM1	DDX1	RPL12	CS	KHSRP	PELO	RPS5	
RPL36A	OTT	DDX5	RPL21	CYLD	LARS	PET112L	RPS6	
RPL37	RPL23	DDX51	RPL22	DARS	LARS2	PLEK	RPS7	
RPL9	RPL3	EBNA1BP2	RPL27	EARS2	MARS	PLEK2	RPS9	
RPS12	RPL37	EBP	RPL28	EEF1A1	MARS2	POLG	RRBP1	
RPS14	RPS11	EMG1	RPL29	EEF1A2	MRPL1	POLG2	RS1	
RPS15	RPS4X	FCF1	RPL3	EEF1B2	MRPL11	POPDC3	RSL1D1	
RPS16	RPS9	FRG1	RPL36A	EEF1D	MRPL12	PTRH1	SARS	
RPS19	RS1	GNL2	RPL37	EEF1E1	MRPL13	QARS	SARS2	
RPS3		GNL3	RPL7A	EEF1G	MRPL14	RARS	SCYE1	
RPS3A		GNL3L	RPL9	EEF2	MRPL15	RARS2	SECISBP2	
RPS4X		GTPBP4	RPS12	EEFSEC	MRPL16	RBM3	SEPSECS	
RPS5		IMP3	RPS14	EIF1A	MRPL17	RPL12	SPP2	
RPS6		IMP4	RPS15	EIF1B	MRPL18	RPL13A	TARS	
RPS6KB1		IPO4	RPS16	EIF2A	MRPL2	RPL18	TARSL2	
RPS7		MRPL1	RPS19	EIF2AK2	MRPL20	RPL19	TNS4	
RPS8		MRPL10	RPS2	EIF2B1	MRPL22	RPL21	TPR	
		MRPL14	RPS24	EIF2B2	MRPL23	RPL22	TSFM	
		MRPL2	RPS3	EIF2B4	MRPL24	RPL22L1	TUFM	
		MRPL22	RPS3A	EIF2B5	MRPL27	RPL23	UBA5	
		MRPL23	RPS4X	EIF2C2	MRPL3	RPL24	UBR1	
		MRPL3	RPS5	EIF2C3	MRPL30	RPL27	VARS	
		MRPL30	RPS6	EIF2C4	MRPL33	RPL27A	VARS2	
		MRPL4	RPS6KA1	EIF2S2	MRPL34	RPL28	WARS	
		MRPS2	RPS6KA3	EIF2S3X	MRPL35	RPL29	WARS2	
		MRPS26	RPS6KB1	EIF3B	MRPL36	RPL3	WDR9	
		MRTO4	RPS7	EIF3D	MRPL39	RPL30		
		NHP2L1	RPS8	EIF3EIP	MRPL4	RPL31		
		NIP7	RRN3	EIF3F	MRPL43	RPL35		
		NOG	SDAD1	EIF3G	MRPL47	RPL36A		
		NOL1		EIF3H	MRPL48	RPL36AL		
				EIF3I	MRPL49	RPL37		
				EIF3K	MRPL51	RPL38		
				EIF4A1	MRPL9	RPL39		
				EIF4A2	MRPS10	RPL3L		
				EIF4B	MRPS11	RPL4		
				EIF4E	MRPS12	RPL41		
				EIF4E2	MRPS14	RPL7A		
				EIF4E3	MRPS15	RPL7L1		
				EIF4G1	MRPS16	RPL9		
				EIF4G2	MRPS17	RPLP1		
				EIF4H	MRPS18A	RPP30		
				EIF5	MRPS18B	RPP38		
				EIF5A	MRPS18C	RPS11		
				EIF6	MRPS2	RPS12		
				EPRS	MRPS21	RPS13		
				ETF1	MRPS30	RPS14		
				FARS2	MRPS5	RPS15		
				FARSA	MRPS6	RPS15A		
				FARSB	MRPS7	RPS16		
				FBXW17	MRPS9	RPS19		
				GARS	MRRF	RPS2		
				GART	MTIF3	RPS21		

Ribosome		Cytosolic Small Ribosomal Subunit	Structural Constituent of Ribosome		RibonucleoProtein Complex				
A	RPL27A	RPS13	A	RPL13A	A	MRPL24	MRPS24	RPL27	RPS7
APEX1	RPL28	RPS14	BC003885	RPL18	CASC3	MRPL27	MRPS25	RPL27A	RPS8
BC003885	RPL29	RPS2	CYLD	RPL19	D10ERTD322E	MRPL28	MRPS26	RPL28	RPS9
CYLD	RPL3	RPS24	FBXW17	RPL21	DAP	MRPL3	MRPS27	RPL29	RPSA
FBXW17	RPL30	RPS4X	MRPL1	RPL22	DAP3	MRPL30	MRPS28	RPL3	RRP9
MRPL1	RPL31	RPS6	MRPL10	RPL22L1	EFTUD2	MRPL33	MRPS30	RPL30	RS1
MRPL11	RPL35	RPS7	MRPL11	RPL23	HNRNPA2B1	MRPL34	MRPS31	RPL31	SNRP70
MRPL12	RPL36A	RPS9	MRPL12	RPL24	HNRNPC	MRPL35	MRPS33	RPL35	SNRPA
MRPL13	RPL36AL	RS1	MRPL13	RPL27	HNRPAB	MRPL36	MRPS34	RPL37	SNRPB
MRPL14	RPL37		MRPL14	RPL27A	HNRPF	MRPL37	MRPS35	RPL38	SNRPB2
MRPL15	RPL38		MRPL15	RPL28	HNRPH1	MRPL38	MRPS5	RPL39	SNRPD1
MRPL16	RPL39		MRPL16	RPL29	HNRPK	MRPL39	MRPS6	RPL3L	SNRPD2
MRPL17	RPL3L		MRPL17	RPL3	HNRPL	MRPL4	MRPS7	RPL4	SNRPD3
MRPL18	RPL4		MRPL18	RPL30	HNRPLL	MRPL40	MRPS9	RPL41	SNRPG
MRPL2	RPL41		MRPL2	RPL31	HNRPM	MRPL43	MVP	RPL7A	SRA1
MRPL20	RPL7A		MRPL20	RPL35	HNRPUL1	MRPL45	NHP2L1	RPL7L1	SRP14
MRPL22	RPL7L1		MRPL22	RPL36A	IMP3	MRPL46	NOLA1	RPL9	SRP19
MRPL24	RPL9		MRPL23	RPL36AL	IMP4	MRPL47	NOLA2	RPLP1	SRP68
MRPL27	RPLP1		MRPL24	RPL37	LARP6	MRPL48	NOLA3	RPLP2	SRP9
MRPL3	RPLP2		MRPL27	RPL38	LSM10	MRPL49	OTT	RPS10	SRPR
MRPL30	RPP30		MRPL3	RPL39	LSM2	MRPL50	PA2G4	RPS11	SRPRB
MRPL33	RPP38		MRPL30	RPL3L	LSM3	MRPL51	PCBP1	RPS12	STAU1
MRPL34	RPS11		MRPL33	RPL4	LSM4	MRPL52	PCBP2	RPS13	SYNC
MRPL35	RPS12		MRPL34	RPL41	LSM5	MRPL53	PCBP3	RPS14	SYNCRIP
MRPL36	RPS13		MRPL35	RPL7A	LSM6	MRPL54	PRMT2	RPS15	TERT
MRPL4	RPS14		MRPL36	RPL7L1	LSM8	MRPL55	PRMT3	RPS15A	TRIM2
MRPL48	RPS15		MRPL39	RPL9	MKRN3	MRPL9	PTBP1	RPS16	TRIM21
MRPL49	RPS15A		MRPL4	RPLP1	MRPL1	MRPS10	PUF60	RPS19	TRO
MRPL9	RPS16		MRPL47	RPLP2	MRPL10	MRPS11	RALY	RPS2	TROVE2
MRPS10	RPS19		MRPL48	RPP30	MRPL11	MRPS12	RBM14	RPS21	U2AF2
MRPS11	RPS2		MRPL49	RPP38	MRPL12	MRPS14	RBMX	RPS24	UBA5
MRPS12	RPS21		MRPL51	RPS10	MRPL13	MRPS15	ROD1	RPS25	YBX2
MRPS14	RPS24		MRPL9	RPS11	MRPL14	MRPS16	RPL12	RPS26	ZCCHC17
MRPS15	RPS26		MRPS10	RPS12	MRPL15	MRPS17	RPL13A	RPS27A	ZRSR2
MRPS16	RPS27A		MRPS11	RPS13	MRPL16	MRPS18A	RPL18	RPS27L	
MRPS17	RPS27L		MRPS12	RPS14	MRPL17	MRPS18B	RPL19	RPS3	
MRPS18A	RPS3		MRPS14	RPS15	MRPL18	MRPS18C	RPL21	RPS3A	
MRPS18B	RPS3A		MRPS15	RPS15A	MRPL2	MRPS2	RPL22	RPS4X	
MRPS18C	RPS4X		MRPS16	RPS16	MRPL20	MRPS21	RPL22L1	RPS5	
MRPS2	RPS4Y2		MRPS17	RPS19	MRPL22	MRPS22	RPL23	RPS6	
MRPS21	RPS5		MRPS18A	RPS2	MRPL23	MRPS23	RPL24	RPS6KL1	
MRPS30	RPS6		MRPS18B	RPS21					
MRPS5	RPS7		MRPS18C	RPS24					
MRPS6	RPS9		MRPS2	RPS26					
MRPS7	RRBP1		MRPS21	RPS27A					
MRPS9	RS1		MRPS22	RPS27L					
NOLA2	RSL1D1		MRPS23	RPS3					
OTT	SECISBP2		MRPS24	RPS3A					
PLEK	SPP2		MRPS25	RPS4X					
PLEK2	SRP68		MRPS26	RPS5					
POPDC3	TG		MRPS30	RPS6					
RPL12	TNS4		MRPS5	RPS6KB1					
RPL13A	UBA5		MRPS6	RPS7					
RPL18	UBR1		MRPS7	RPS8					
RPL19			MRPS9	RPS9					
RPL21			NOLA2	RS1					
RPL22			OTT	RSL1D1					
RPL22L1			PLEK	SECISBP2					
RPL23			PLEK2	SPP2					
RPL24			POPDC3	TNS4					
RPL27			RPL12	UBA5					
				UBR1					

Fig. S8, related to Fig. 4B. **Gene list of protein translation-related clusters**. The list of genes in each cluster from the gene ontology analysis in Fig.4B is shown.

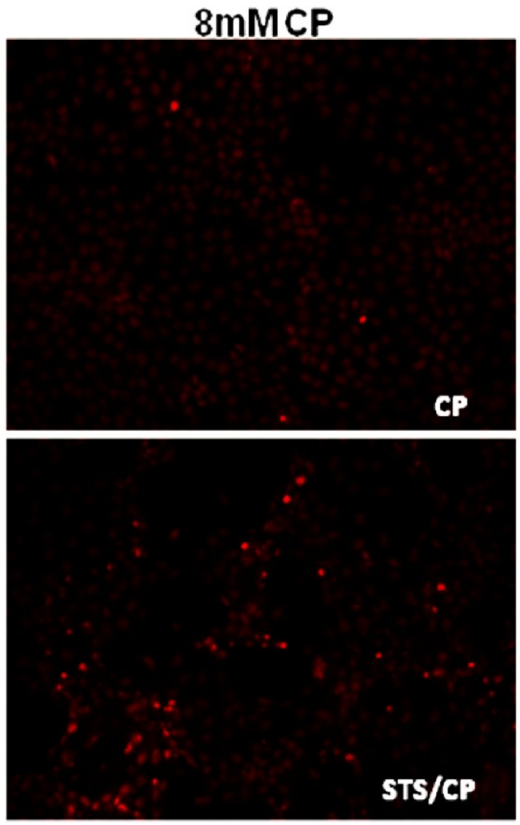

Fig. S9, related to Fig. 5D. **Effect of starvation on CP-induced intracellular superoxide levels**. Murine breast cancer cells (4T1) were fasted and treated with CP in vitro. Superoxide levels were estimated by DHE (dihydroethidium) staining. (10x magnification).